双控石墨烯超材料太赫兹调制器的双频反射特性

张玉萍，吕欢欢，李彤彤，张会云

（山东科技大学 电子通信与物理学院，山东 青岛 266590）

摘　要： 设计了双控太赫兹超材料调制器，并研究了其在太赫兹频段内两个频率处的反射特性。该调制器由开口环谐振器及其底部的“三明治”结构组成，“三明治”结构从上到下依次为石墨烯层、聚酰亚胺层和金层，其中开口谐振器的开口处填充硅。该结构可以通过电、光两种方式调制，即分别对调制器中的石墨烯施加低电压，对硅施加弱光照。结果显示：反射谱在频率 0.806 THz、1.869 THz 出现两个共振反射谷，在满足低激励的条件下，增强两种激励均能改变共振反射谷的反射强度。两个共振处的反射调制方向表现出先反向、后同向的特点，其临界点对应的石墨烯费米能级和硅电导率分别为 13.489 meV、970.54 S/m。文章对同时施加两种激励的情况进行了详细研究，结果表明：同时施加两种激励的调制特性并非单独施加激励的数值叠加，电、光两种调制方式相互独立。在调制过程中，调制器出现的最大调制深度为 99.74%。

关键词： 双控；石墨烯；太赫兹反射调制器；弱激励；强调制

中图分类号： O433　　**文献标志码：** A　　**文章编号：** 1672-3767(2016)06-0068-08

Reflection Modulation Properties at Two Frequencies of Dual-control Graphene Metamaterial Terahertz Modulator

ZHANG Yuping，LÜ Huanhuan，LI Tongtong，ZHANG Huiyun

（College of Electronics，Communication and Physics，Shandong University of Science and Technology，Qingdao，Shandong 266590，China）

Abstract： A dual-control terahertz metamaterial modulator was proposed，whose reflection properties at two frequencies in the terahertz frequency range can be tuned by voltage and illumination. The metamaterial modulator is composed of a split-ring resonator，which is deposited on a sandwich structure of a graphene layer，a polyimide spacer layer and a gold layer，embedded by semiconductor silicon in the split gap. The study was achieved by applying low bias voltage on graphene layer and weak light intensity on semiconductor，respectively. The results demonstrate two reflection dips in the reflective spectrum，moreover，both excitations can change the strength of resonance reflection dip. The resonance reflection dip at 0.806 THz rises with the increasing of the Fermi level or the light intensity. While at 1.869 THz，the resonance reflection dip first decreases and then increases，reaches its minimum at Fermi level of 13.489 meV and light pump of 970.54 S/m，respectively. Numerical results with two external stimuli changing simultaneously are also presented. The best amplitude modulation depth that could be achieved is 99.74% at 0.806 THz with the Fermi level changes from 0.2 meV to 60 meV.

Key words： dual-control；graphene；THz reflection modulation；weak excitation；strong modulation

PACS： 01.10.Hx，02.60.Cb，61.48.Gh，61.82.Fk

收稿日期： 2016-05-25

基金项目： 国家自然科学基金项目(61001018)；山东省自然科学基金项目(ZR2016FM09)；山东省高等学校科技计划项目(J13LN16)；青岛市创新领军人才项目(13-CX-25)；中国工程物理研究院太赫兹科学技术基金项目(201401)；青岛经济技术开发区重点科技计划项目(2013-1-64)；山东科技大学研究生创新基金项目(YC150354)

作者简介： 张玉萍(1976—)，女，山东日照人，副教授，硕士生导师，主要从事太赫兹技术和超材料方面的研究工作.
E-mail：sdust_thz@163.com

High speed modulators are very important components in electromagnetic fields because of their usefulness in modulated lasers, construction of the on-chip interconnects in communication system[1-3], and data transmission for biomedical implanted devices[4]. Metamaterials, which are designable for their unusual and exotic electromagnetic properties, have advantages in controlling radiation at microwave, terahertz, infrared and optical frequencies [5-15]. In THz field, several groups achieved active manipulation of metamaterials by applying electrical control[6,16] or optical illumination[17-19]. Semiconductors such as Si and GaAs could be incorporated into metamaterial to form hybrid structures which could be tuned by optical external stimulus that modify the carrier dynamics of the semiconductor inclusions [6,20-21]. Graphene, consisting of one monolayer of carbon atoms arranged in a honeycomb lattice, is a promising candidate for designing gate-controlled modulator due to the properties of electrostatic control of conductivity[11,16,22-24]. Therefore, it would be intriguing to incorporate semiconductor and graphene into the metamaterials[25] to provide better THz modulation performance.

Compared to transmission modulators that are paid more attention[16,22,26-27], reflection modulators could reduce the insertion loss and show significance especially in the development of THz communication system. But there are only few reports about THz reflection modulation so far[28-29], which show modulating properties at a single frequency. In addition, high external gate voltage (850 V) is often needed in many gate-controlled modulators consisting of graphene metamaterial[11], while it is highly desirable to realize giant modulation with weak external excitation for practical application[13,15].

In this article, we propose a design and numerical study of a dual-control metamaterial terahertz reflection modulatorand study its reflection modulation properties at two frequencies. The four-layer metamaterial modulator composes of split-ring resonators deposited on a graphene layer and with semiconductor silicon embedded in the split gap, a polyimide spacer layer in the middle and a metallic layer in the bottom. We accomplish our study by applying low bias voltage on graphene layer and weak light intensity on semiconductor, respectively. The modulation mechanism is analyzed theoretically.

1 Design and simulation

The structure of the metamaterial modulator is illustrated in Fig.1. The parameters were referenced[30]. The structure of the modulator is a four-layer-sandwich that is similar to an absorber. The bottom layer is a 200-nm-thick gold layer, with a 6.5-μm-thick polyimide layer on top of it acts as the spacer. A

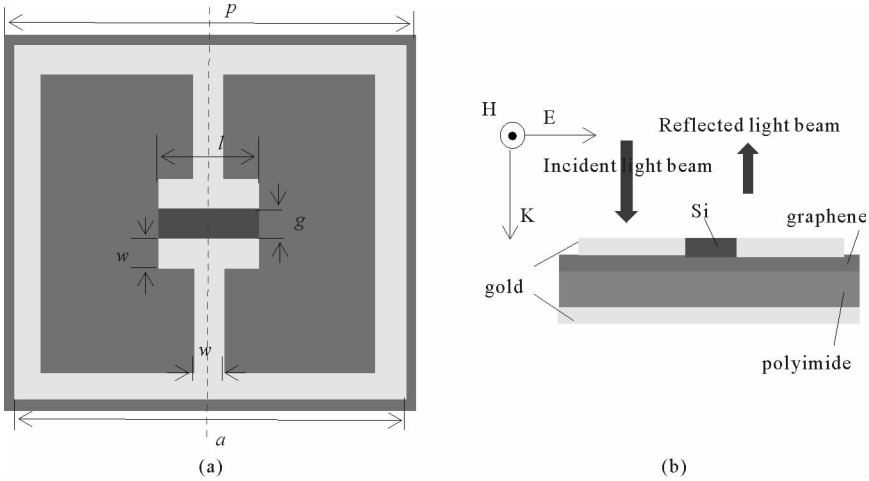

Fig. 1 The schematic diagram of the dual-control metamaterial terahertz modulator(a), the cutaway views of the modulator(b). p=40.8 μm, a=40 μm, l=14 μm, w=3 μm and g=4 μm. the polarization of the normally incident wave was labeled

0.5-nm-thick graphene monolayer spread over the spacer. The top layer structure is periodically arranged split-ring resonators with thickness of 200 nm. The gap of the split-ring resonators was inserted by silicon.

The gold is modeled as loss metal with electric conductivity $\sigma_{\text{gold}}=4.09\times10^{7}$ S/M. The polyimide is simulated with the dielectric constant $\varepsilon_{\text{polyimide}}=2.9$ and loss tangent(δ)=0.02. The characteristic parameter of the graphene can be well-described by a Drude model [31-35] and its conductivity is defined as

$$\sigma=\frac{2e^{2}\varepsilon_{F}}{\pi\hbar^{2}\mathrm{k_B}T}\cdot\frac{i}{(\omega+i\tau^{-1})}\cdot\ln\left(2\cosh\left(\frac{\varepsilon_{F}}{2\mathrm{k_B}T}\right)\right). \tag{1}$$

where ε_F is the Fermi level of graphene, the relaxation rate is $\tau=\frac{\mu\varepsilon_F}{ev_F^2}$ with the mobility $\mu=10^4$ cm^{2}V^{-1}s^{-1} and Fermi velocity $v_F=10^6$ m/s, Boltzmann constant k_B and the temperature $T=300$ K.

In our simulations, we vary the conductivity of the photoconductive silicon and Fermi level of electric-pumped graphene to gain the dual-control reflection modulator. The simulations of the metamaterial terahertz reflection modulator were performed by using the finite difference time domain(FDTD) method.

2 Results and discussion

2.1 The stimulated results without external stimuli

We first study the reflective spectrum of the THz reflection modulator without illumination and bias voltage, shown in Fig. 2. We define the conductivity of silicon $\sigma_{si}=1$ S/m as no illumination, and reduce the Fermi level of graphene to 0.2 meV as no bias voltage. This is because the Fermi level of graphene cannot be reduced unlimitedly in Drude model. The results demonstrate the two reflection dips correspond to 0.806 and 1.869 THz respectively. The reflective value at 0.806 THz is 0.22%, and 22.57% at 1.869 THz. In order to describe the mechanism of the two cases, we exhibit the current density distribution of low and higher frequency dips in Fig. 3 (a, b), (c, d) respectively. When the electromagnetic wave incidents into the metamaterial modulator normally, the wave is first reflected and transmitted at the SRR resonator arrays, and then the surface current of the SRR is generated. The transmitted wave is reflected by the ground gold layer, generating surface current in the bottom gold layer. Figure 3 shows that the current direction of the SRR resonator is opposite to that of ground gold layer.

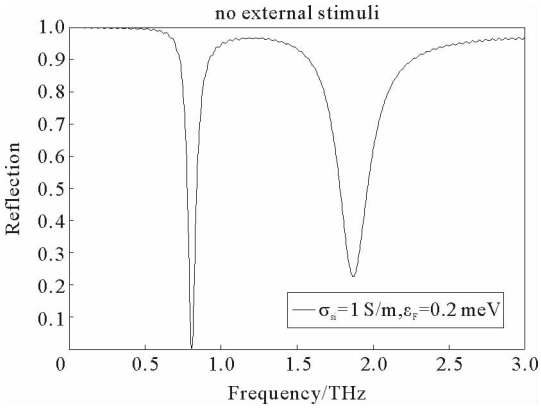

Fig. 2 The reflective spectrum of the THz reflection modulator without external stimuli

For the 0.806 THz resonance, it is evident that in the plane of the electric resonator (SRR) there are counter-circulating currents which are associated with the LC resonance. In addition, there is also a magnetic response associated with a circulating displacement current between the SRR and the ground plane. Thus the combined effect of the electric and magnetic response leads to the resonance at 0.806 THz. In contrast, resonance at the 1.869 THz is determined solely by the magnetic response which drives the circulating displacement current between the resonator and ground plane. This frequency response is analogous to what has previously been observed using similar surface at higher frequencies[36-38].

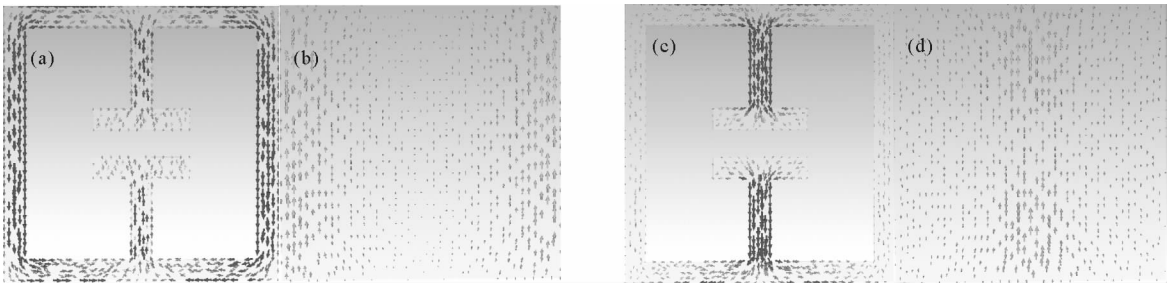

Fig. 3 Current density of the (a) SRR and (b) ground gold at resonance frequency 0.806 THz, current density of the (c) SRR and (d) ground gold at resonance frequency 1.869 THz

2.2 Electronically control

Unlike the previous work, in our simulation, we employ low Fermi level from 0.2 meV to 60 meV to study the modulation properties of the device, shown in Fig. 4. With the increasing of the Fermi level of graphene, the reflective value at 0.806 THz increases, while the dip at 1.869 THz decreases from 0.2 meV to 13.489 meV, but then increases from 13.489 meV to 60 meV accompanied by frequency blue-shift.

Analogous to the definition of transmission modulation depth[27], for the 0.806 THz the reflectance modulation depth is defined as $|(R_i - R_0)/R_i| \times 100\%(i = \sigma_{si}, \varepsilon_F)$, for the 1.869 THz resonance, the reflectance modulation depth is defined as $|(R_0 - R_i)/R_0| \times 100\%(i = \sigma_{si}, \varepsilon_F)$, where R_i refers to the reflection value of the dip when the Fermi level or silicon conductivity changes, R_0 stands for the reflection value without the external stimuli.

The modulation depth controlled electrically reaches 99.58% at 0.806 THz and 99.61% at 1.869 THz with opposite modulating direction, when the Fermi level changes from 0.2 meV to 13.489 meV. With the Fermi level increase from 13.489 meV further to 60 meV, the modulation depth at the first dip 0.806 THz reaches 99.74% and the maximum reflection rate increased to 87.82%, this is beneficial to reduce the loss in the practical application. Blue-shift appears at the resonance of 1.869 THz when the Fermi level increases from 13.489 meV to 60 meV. Especially, at 2.16 THz, the modulation depth between 0.2 meV and 60 meV reaches 59.58%, and the reflection value is larger than that at other Fermi level, leading to less loss, so it is practical for the modulation of light and the optical information processing.

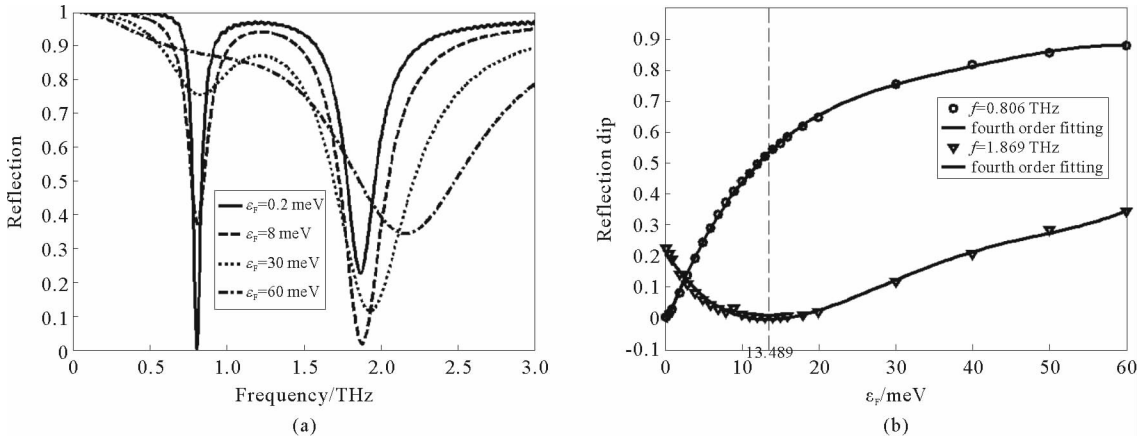

Fig. 4 The reflective spectrum with the Fermi level increasing(a), the Fermi level dependent reflection at the dips of the reflective spectrum(b)

In order to observe the Fermi level dependent reflection spectrum dip intuitively, in Fig. 4, we plot the curve between Fermi level and reflection dip for the two dips near 0.806 THz and 1.869 THz, and found that the data meets the fourth order fitting.

To look into the mechanism of the modulation, we make an analysis about the two dips changing with the electric excitation. For resonance at the 0.806 THz, it is a combined effect of the electric and magnetic response. The electric bias voltage acts on the graphene changes the carrier density in the graphene, thus changes the Fermi level of the graphene. With the Fermi level increases from 0.2 meV to 60 meV, the conductivity of the graphene increases approximately nearly from $3.236\,2\times10^{-5}+i1.854\,0\times10^{-9}$ to $4.271\,7\times10^{-4}+i1.906\,2\times10^{-4}$, according to $\varepsilon_{\text{eff}}=1+\frac{i\sigma}{\omega\varepsilon_0 d}$ [39], the real part of the effective graphene permittivity $\text{Re}(\varepsilon_{\text{eff}})$ changes from 0.961 9 to $-5.681\,7\times10^{3}$, thus the conduction rate of the graphene under the gap of the SRR increases, making the capacitor smaller, the LC oscillation of the SRR weaker and the reflection of the device stronger. The enhancement of the magnetic response can be neglected compared to the change in LC oscillation of the SRR. As a whole, the reflection of the first dip increases with the Fermi level.

The resonance at 1.869 THz is determined solely by the magnetic response which drives the circulating displacement current between the resonator and ground plane. When the Fermi level increase from 0.2 meV to 13.489 meV, the frequency ($\omega_P\propto\sqrt{\sigma}$) of the plasma increases and approaches the frequency of the dipole of the magnetic response. Resonance is produced, thus energy dissipated inside the device increases and reflection of the device decreases. With the Fermi level increasing further, the frequency of the plasma increases and departs gradually from the frequency of the dipole of the magnetic response, making the reflection of the first dip rise.

According to the static model of large-area single graphene layer nonuniformity[24,39], the Fermi level can be described :

$$|\varepsilon_F(V_g)|=\hbar v_f\sqrt{\pi\alpha_c|V_g-\widetilde{V}_{\text{CNP}}|}。\tag{2}$$

where $\varepsilon_F(V_g)$ is the fermi level at gate voltage V_g, $\hbar$ is the reduced plank constant, v_f is the fermi level, α_c is a capacitor constant($\alpha_c\approx2.4\times10^{11}\ \text{cm}^{-2}\text{V}^{-1}$), and $\widetilde{V}_{\text{CNP}}$ is the voltage shifting the fermi level of graphene to the Dirac point($\widetilde{V}_{\text{CNP}}\approx-14\ V$). On the basis of equation (2), 60 meV of fermi level corresponds to −12.9 V of gate voltage, which is lower than 850 V mentioned in ref. [11].

3.3 Optically control

The other way of realizing reflection modulation is to optically pump the silicon. In this article, we use the variation of the silicon conductivity to stand for the change of optical pump. Fortunately, weak change of optical pump (conductivity of silicon) can excite modulation in the reflection spectrum, which was not shown in other researches. In Fig. 5(a), keeping the Fermi level of graphene 0.2 meV still, we calculate the reflective spectrum, when the conductivity of silicon changes from 1 to 6 000 S/m. the strength of reflection increases from 0.22% to 56.68% at 0.806 THz.

We also plot silicon conductivity dependent reflection at the dip, in Fig. 5(b). The reflection features is proportional to the intensity of external stimuli at 0.806 THz, while the reflection at 1.869 THz weaken with the increasing external excitation. The fitting result of the silicon conductivity dependent reflection dip show the data meets the fifth order fitting. The maximum of reflectance modulation depth reaches 99.68% and 97.01% at the resonance frequencies of 0.806 THz and 1.869 THz, respectively.

The principle of the resonance at two frequencies in the optical way is the same as that in the electrical way. For the resonance at 0.806 THz, with the conductivity of silicon increasing, the photo-induced carriers increase, and then the gap of the SRR is shorted, as a result, the LC resonance of SRR is weakening. During

this process, the change of the magnetic coupling between SRR and gold layer in the bottom is small enough to be ignored. On the whole, the conductivity of silicon increase process is the weakening process of the 0.806 THz resonance.

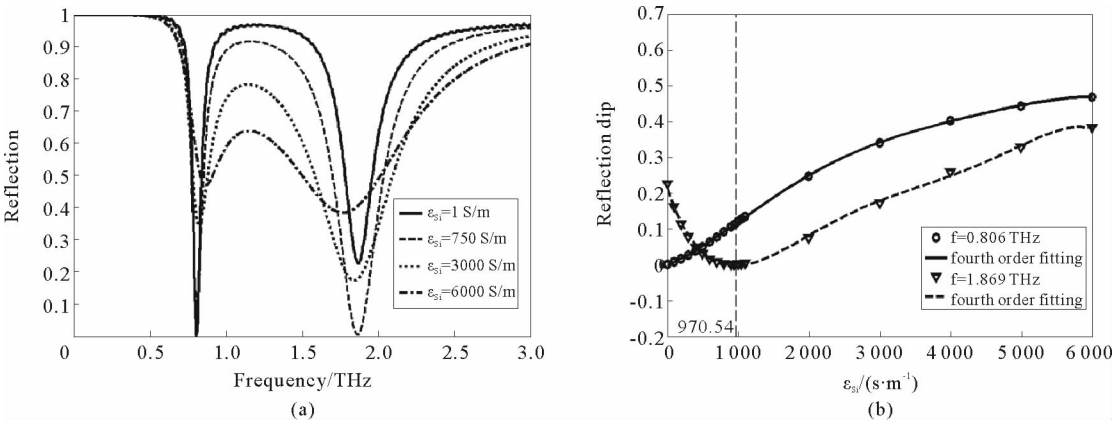

Fig. 5 The reflective spectrum with the silicon conductivity increasing(a), the silicon conductivity dependent reflection at the dips of the reflective spectrum(b)

On the other hand, the photo-induced carriers diffuse from silicon to graphene and the Fermi level of graphene increases ($\varepsilon_F = \hbar v_F \sqrt{\pi |n|}$), resulting in the change of the graphene conductivity. Corresponding, the plasma frequency approaches the oscillation frequency of the magnetic dipole gradually and then resonance occurs while the conductivity of silicon changes from 1 to 970.54 S/m. The intensity of resonance between plasma and magnetic dipole reaches maximum, at σ_{Si} = 970.45 S/m. Increase the silicon conductivity to 6 000 S/m, the frequency of plasma departs from the oscillation frequency of the magnetic dipole, and the resonance between them weakens.

In particular, the light conductivity of semiconductor in steady state can be expressed [40]:

$$\sigma_{Si} = q\beta\alpha(\mu_n\tau_n + \mu_p\tau_p) \cdot I, \tag{3}$$

where q is the electron charge, β , α characterize the interaction between light and matter, μ , τ indicate the interaction between carriers and matter, and I is the intensity of light. The equation (3) shows photo-conductivity is proportional to light intensity. So the conductivity of silicon determines the high light intensity is unnecessary in this study.

In the last of this paper, we try to exert the two stimuli on the metamaterial simultaneously, to look forward to more modulation depth. We plot the figure 6 and the result is not agreed with our expectation. For the resonance at 0.806 THz, although the simultaneous application of the two stimuli makes the photo-induced carriers increase quickly, the enhancement to the LC resonance of SRR is offset by weakening capacity of the gap to a great degree. Therefore, the resonance intensity of simultaneously applying the two stimuli do not equal to the algebraic sum of the resonance intensity

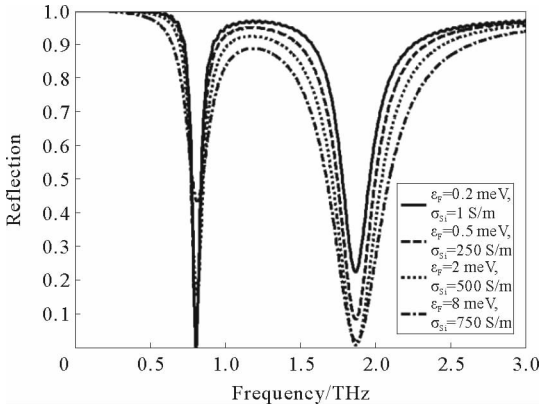

Fig. 6 The reflective spectrum with optical and electrical stimuli coexisting

while exerting one stimulus. Similarly, for the resonance at 1.869 THz, simultaneous application of the two stimuli do not contribute to the double intensity of the magnetic response of the plasma and the dipole. The results indicate that the modulator can be controlled electrically or optically independently.

4 Conclusion

In summary, we demonstrate the modulating properties at two frequencies in the THz range by using a dual-control metamaterial THz modulator with weak external excitation. The increase of graphene Fermi level and the conductivity of silicon both generate modulation effects in the device. Two reflection dips at 0.806 THz and 1.869 THz appear in the reflection spectrum. The dip at 0.806 THz rises while the dip at 1.869 THz first falls and then rises with the intensity of excitation increasing. They show opposite modulation properties with Fermi level changes from 0.2 meV to 13.489 meV when electrically pumped and with conductivity of silicon changes from 1 to 970.54 S/m when optically pumped. In addition, we also calculate the reflection modulation spectrum with two excitations changed at the same time, and the result indicates the two controlled way can be carried out independently. This design will benefit the flexibility in the application of metamaterial and the development of the future application in THz communication, imaging, and sensing.

References:

[1]MILLER D A B. Are optical transistors the logical next step? [J]. Nature Photonics, 2010, 4(1): 3-5.

[2]REED G T, MASHANOVICH G, GARDES F Y, et al. Silicon optical modulators[J]. Nature Photonics, 2010, 4(8): 518-526.

[3]WEN Q Y, TIAN W, MAO Q, et al. Graphene based all-optical spatial terahertz modulator[J]. Scientific Reports, 2014, 4: 7409.

[4]HANNAN M A, ABBAS S M, SAMAD S A, et al. Modulation techniques for biomedical implanted devices and their challenges[J]. Sensors, 2011, 12(1): 297-319.

[5]VALENTINE J, LI J, ZENTGRAF T, et al. An optical cloak made of dielectrics[J]. Nature Materials, 2009, 8(7): 568-571.

[6]PENDRY J B. Negative refraction makes a perfect lens[J]. Physical Review Letters, 2000, 85(18): 3966.

[7]KABASHIN A V, EVANS P, PASTKOVSKY S, et al. Plasmonic nanorod metamaterials for biosensing[J]. Nature Materials, 2009, 8(11): 867-871.

[8]CHEN H T, PADILLA W J, ZIDE J M O, et al. Active terahertz metamaterial devices[J]. Nature, 2006, 444(7119): 597-600.

[9]LEE S H, CHOI M, KIM T T, et al. Switching terahertz waves with gate-controlled active graphene metamaterials[J]. Nature Materials, 2012, 11(11): 936-941.

[10]MOUSAVI S H, KHOLMANOV I, ALICI K B, et al. Inductive tuning of Fano-resonant metasurfaces using plasmonic response of graphene in the mid-infrared[J]. Nano Letters, 2013, 13(3): 1111-1117.

[11]VALMORRA F, SCALARI G, MAISSEN C, et al. Low-bias active control of terahertz waves by coupling large-area CVD graphene to a terahertz metamaterial[J]. Nano Letters, 2013, 13(7): 3193-3198.

[12]PIPER J R, FAN S. Total absorption in a graphene monolayer in the optical regime by critical coupling with a photonic crystal guided resonance[J]. ACS Photonics, 2014, 1(4): 347-353.

[13]DEGL'INNOCENTI R, JESSOP D S, SHAH Y D, et al. Low-bias terahertz amplitude modulator based on split-ring resonators and graphene[J]. ACS Nano, 2014, 8(3): 2548-2554.

[14]DOLLING G, ENKRICH C, WEGENER M, et al. Low-loss negative-index metamaterial at telecommunication wavelengths [J]. Optics Letters, 2006, 31(12): 1800-1802.

[15]GUPTA S, CALOZ C. Analog Signal Processing in Transmission Line Metamaterial Structures[J]. Radioengineering, 2009, 18(2).

[16]YAN R, SENSALE-RODRIGUEZ B, LIU L, et al. A new class of electrically tunable metamaterial terahertz modulators [J]. Optics Express, 2012, 20(27): 28664-28671.

[17]PADILLA W J, TAYLOR A J, HIGHSTRETE C, et al. Dynamical electric and magnetic metamaterial response at terahertz

frequencies[J]. Physical Review Letters,2006,96(10):107401.

[18]GU J,SINGH R,LIU X,et al. Active control of electromagnetically induced transparency analogue in terahertz metamaterials[J]. Nature Communications,2012,3:1151.

[19]FAN K,STRIKWERDA A C,ZHANG X,et al. Three-dimensional broadband tunable terahertz metamaterials[J]. Physical Review B,2013,87(16):161104.

[20]XU Z C,GAO R M,DING C F,et al. Photoexcited broadband blueshift tunable perfect terahertz metamaterial absorber[J]. Optical Materials,2015,42:148-151.

[21]SHREKENHAMER D,ROUT S,STRIKWERDA A C,et al. High speed terahertz modulation from metamaterials with embedded high electron mobility transistors[J]. Optics Express,2011,19(10):9968-9975.

[22]SENSALE-RODRIGUEZ B,YAN R,KELLY M M,et al. Broadband graphene terahertz modulators enabled by intraband transitions[J]. Nature Communications,2012,3:780.

[23]LI J,ZHOU Y,QUAN B,et al. Graphene-metamaterial hybridization for enhanced terahertz response[J]. Carbon,2014,78:102-112.

[24]REN L,ZHANG Q,YAO J,et al. Terahertz and infrared spectroscopy of gated large-area graphene[J]. Nano Letters,2012,12(7):3711-3715.

[25]LI Q,TIAN Z,ZHANG X,et al. Active graphene-silicon hybrid diode for terahertz waves[J]. Nature Communications,2015,6.

[26]WEIS P,GARCIA-POMAR J L,Hoöh M,et al. Spectrally wide-band terahertz wave modulator based on optically tuned graphene[J]. ACS Nano,2012,6(10):9118-9124.

[27]LI Q,TIAN Z,ZHANG X,et al. Dual control of active graphene-silicon hybrid metamaterial devices[J]. Carbon,2015,90:146-153.

[28]ZHU W,RUKHLENKO I D,PREMARATNE M. Graphene metamaterial for optical reflection modulation[J]. Applied Physics Letters,2013,102(24):241914.

[29]SENSALE-RODRIGUEZ B,YAN R,RAFIQUE S,et al. Extraordinary control of terahertz beam reflectance in graphene electro-absorption modulators[J]. Nano Letters,2012,12(9):4518-4522.

[30]CHEN H T,O'HARA J F,AZAD A K,et al. Experimental demonstration of frequency-agile terahertz metamaterials[J]. Nature Photonics,2008,2(5):295-298.

[31]KOPPENS F H L,CHANG D E,GARCIA DE ABAJO F J. Graphene plasmonics:A platform for strong light-matter interactions[J]. Nano Letters,2011,11(8):3370-3377.

[32]LI Z Q,HENRIKSEN E A,JIANG Z,et al. Dirac charge dynamics in graphene by infrared spectroscopy[J]. Nature Physics,2008,4(7):532-535.

[33]WANG F,ZHANG Y,TIAN C,et al. Gate-variable optical transitions in graphene[J]. Science,2008,320(5873):206-209.

[34]DOCHERTY C J,JOHNSTON M B. Terahertz properties of graphene[J]. Journal of Infrared,Millimeter,and Terahertz Waves,2012,33(8):797-815.

[35]HORNG J,CHEN C F,GENG B,et al. Drude conductivity of Dirac Fermions in graphene[J]. Physical Review B,2011,83(16):165113.

[36]TAO H,BINGHAM C M,STRIKWERDA A C,et al. Highly flexible wide angle of incidence terahertz metamaterial absorber:Design,fabrication,and characterization[J]. Physical Review B,2008,78(24):241103.

[37]SIEVENPIPER D,ZHANG L,BROAS R F J,et al. High-impedance electromagnetic surfaces with a forbidden frequency band[J]. IEEE Transactions on Microwave Theory and Techniques,1999,47(11):2059-2074.

[38]HAO J M,ZHOU L,CHAN C T. An effective-medium model for high-impedance surfaces[J]. Applied Physics A,2007,87(2):281-284.

[39]GAO W,SHU J,REICHEL K,et al. High-contrast terahertz wave modulation by gated graphene enhanced by extraordinary transmission through ring apertures[J]. Nano Letters,2014,14(3):1242-1248.

[40]XU Z,GAO R,DING C,et al. Photoexited switchable metamaterial absorber at terahertz frequencies[J]. Optics Communications,2015,344:125-128.

(责任编辑:李　磊)